

Numerical Study of Cosmological Singularities

Beverly K. Berger, David Garfinkle
Physics Department, Oakland University, Rochester, MI 48309 USA

Vincent Moncrief
Physics Department, Yale University, New Haven, CT 06520 USA

June 1, 2018

Abstract

The spatially homogeneous, isotropic Standard Cosmological Model appears to describe our Universe reasonably well. However, Einstein's equations allow a much larger class of cosmological solutions. Theorems originally due to Penrose and Hawking predict that all such models (assuming reasonable matter properties) will have an initial singularity. The nature of this singularity in generic cosmologies remains a major open question in general relativity. Spatially homogeneous but possibly anisotropic cosmologies have two types of singularities: (1) velocity dominated—(reversing the time direction) the universe evolves to the singularity with fixed anisotropic collapse rates ; (2) Mixmaster—the anisotropic collapse rates change in a deterministically chaotic way. Much less is known about spatially inhomogeneous universes. Belinskii, Khalatnikov, and Lifshitz (BKL) claimed long ago that a generic universe would evolve toward the singularity as a different Mixmaster universe at each spatial point. We shall report on the results of a program to test the BKL conjecture numerically. Results include a new algorithm to evolve homogeneous Mixmaster models, demonstration of velocity dominance and understanding of evolution toward velocity dominance in the plane symmetric Gowdy universes (spatial dependence in one direction), demonstration of velocity dominance in polarized U(1) symmetric cosmologies (spatial dependence in two directions), and exploration of departures from velocity dominance in generic U(1) universes.

1 Introduction

We shall describe a series of numerical studies of the nature of singularities in cosmological models. Since the interiors of black holes can be described locally as cosmological models, it is possible that our methods and results may be useful to the participants in this conference.

The generic singularity in spatially homogeneous cosmologies is reasonably well understood. The approach to it asymptotically falls into two classes. The first, called asymptotically velocity term dominated (AVTD) [1, 2], refers to a cosmology that approaches the Kasner (vacuum, Bianchi I) solution [3] as $\tau \rightarrow \infty$. (Spatially homogeneous universes can be described as a sequence of homogeneous spaces labeled by τ . Here we shall choose τ so that $\tau = \infty$ coincides with the singularity.) An example of such a solution is the vacuum Bianchi II model [4] which begins with a fixed set of Kasner-like anisotropic expansion rates, and, possibly, makes one change of the rates in a prescribed way (Mixmaster-like bounce) and then continues to $\tau = \infty$ as a fixed Kasner solution. In contrast are the homogeneous cosmologies which display Mixmaster dynamics such as vacuum Bianchi VIII and IX [5, 6, 7] and Bianchi VI₀ and Bianchi I with a magnetic field [8, 9, 10]. Jantzen [11] has discussed other examples. Mixmaster dynamics describes an approach to the singularity which is a sequence of Kasner epochs with a prescription, originally due to Belinskii, Khalatnikov, and Lifshitz (BKL) [5], for relating one Kasner epoch to the next. Some of the Mixmaster bounces (era changes) display sensitivity to initial conditions one usually associates with chaos and in fact Mixmaster dynamics is chaotic [12]. The vacuum Bianchi I (Kasner) solution is distinguished from the other Bianchi types in that the spatial scalar curvature 3R , (proportional to) the minisuperspace (MSS) potential [6, 13], vanishes identically. But 3R arises in other Bianchi types due to spatial dependence of the metric in a coordinate basis. Thus an AVTD singularity is also characterized as a regime in which terms containing or arising from spatial derivatives no longer influence the dynamics. This means that the Mixmaster models do not have an AVTD singularity since the influence of the spatial derivatives (through the MSS potential) never disappears—there is no last bounce.

In the late 1960's, BKL claimed to show that singularities in generic solutions to Einstein's equations are locally of the Mixmaster type [5]. This means that each point of a spatially inhomogeneous universe could collapse to the singularity as the Mixmaster sequence of Kasner models. (It has been argued that this could generate a fractal spatial structure [15, 16, 17].) In contrast, each point of a cosmology with an AVTD singularity evolves asymptotically as a fixed Kasner model. Although the BKL result is controversial [14], it provides a hypothesis for testing. Our ultimate objective is to test the BKL conjecture numerically.

2 Numerical Methods

The work reported here was performed by using symplectic ODE and PDE solvers [18, 19]. While other numerical methods may be used to solve Einstein's equations for the models discussed here, symplectic methods have proved extremely advantageous for Mixmaster models and have also worked quite well in the Gowdy plane symmetric and polarized $U(1)$ symmetric cosmologies [20, 21,

22, 23]. Consider a system with one degree of freedom described by $q(t)$ and its canonically conjugate momentum $p(t)$ with a Hamiltonian

$$H = \frac{p^2}{2m} + V(q) = H_K + H_V. \quad (1)$$

Note that the subhamiltonians H_K and H_V separately yield equations of motion which are exactly solvable no matter the form of V . Variation of H_K yields $\dot{q} = p/m$, $\dot{p} = 0$ with solution

$$p(t + \Delta t) = p(t) \quad , \quad q(t + \Delta t) = q(t) + \frac{p(t)}{m} \Delta t. \quad (2)$$

Variation of H_V yields $\dot{q} = 0$, $\dot{p} = -dV/dq$ with solution

$$q(t + \Delta t) = q(t) \quad , \quad p(t + \Delta t) = p(t) - \left. \frac{dV}{dq} \right|_t \Delta t. \quad (3)$$

Note that the absence of momenta in H_V makes (3) exact for any $V(q)$. One can then demonstrate that to evolve from t to $t + \Delta t$ an evolution operator $\mathcal{U}_{(2)}(\Delta t)$ can be constructed from the evolution sub-operators $\mathcal{U}_K(\Delta t)$ and $\mathcal{U}_V(\Delta t)$ obtained from (2) and (3). One can show that [18]

$$\mathcal{U}_{(2)}(\Delta t) = \mathcal{U}_K(\Delta t/2) \mathcal{U}_V(\Delta t) \mathcal{U}_K(\Delta t/2) \quad (4)$$

reproduces the true evolution operator through order $(\Delta t)^2$. Suzuki has developed a prescription to represent the full evolution operator to arbitrary order [24]. For example

$$\mathcal{U}_{(4)}(\Delta t) = \mathcal{U}_{(2)}(s\Delta t) \mathcal{U}_{(2)}[(1-2s)\Delta t] \mathcal{U}_{(2)}(s\Delta t) \quad (5)$$

where $s = 1/(2 - 2^{1/3})$. The advantage of Suzuki's approach is that one only needs to construct $\mathcal{U}_{(2)}$ explicitly. $\mathcal{U}_{(2n)}$ is then constructed from appropriate combinations of $\mathcal{U}_{(2n-2)}$.

The generalization of this method to N degrees of freedom and to fields is straightforward. In the latter case, $V[\vec{q}(t)] \rightarrow V[\vec{q}(\vec{x}, t)]$ so that dV/dq becomes the functional derivative $\delta V/\delta q$. On the computational spatial lattice, the derivatives that are obtained in the expression for the functional derivative must be represented in differenced form. We note that, to preserve n th order accuracy in time, n th order accurate spatial differencing is required. Some discussion of this has been given elsewhere [21].

3 Application to Mixmaster Dynamics

(Diagonal) Bianchi Class A cosmologies [13] are described by the metric

$$ds^2 = -e^{3\Omega} dt^2 + (e^{2\beta})_{ij} \sigma^i \sigma^j \quad (6)$$

where $\beta_{ij} = \text{diag}(-2\beta_+, \beta_+ + \sqrt{3}\beta_-, \beta_+ - \sqrt{3}\beta_-)$, $d\sigma^i = C_{jk}^i \sigma^j \wedge \sigma^k$ defines the Bianchi type and t is the BKL time coordinate. Einstein's equations can be obtained by variation of the Hamiltonian

$$2H = -p_\Omega^2 + p_+^2 + p_-^2 + V(\beta_+, \beta_-, \Omega). \quad (7)$$

The logarithmic anisotropic scale factors α , ζ , and γ are given in terms of the logarithmic volume Ω and anisotropic shears β_\pm as

$$\begin{aligned} \alpha &= \Omega - 2\beta_+, \\ \zeta &= \Omega + \beta_+ + \sqrt{3}\beta_-, \\ \gamma &= \Omega + \beta_+ - \sqrt{3}\beta_-. \end{aligned} \quad (8)$$

The momenta p_Ω , p_\pm are canonically conjugate to Ω , β_\pm respectively. For vacuum Bianchi IX or magnetic Bianchi VI₀, the MSS potential V has the form [20]

$$V = c^2 e^{2b\alpha} + e^{4\zeta} + e^{4\gamma} - 2 \left(a e^{2(\alpha+\zeta)} + a e^{2(\alpha+\gamma)} + d e^{2(\zeta+\gamma)} \right). \quad (9)$$

Here $a = 1$, $b = 2$, $c = 1$, and $d = 1$ for vacuum Bianchi Type IX, while $a = 0$, $b = 1$, $c = \sqrt{\xi}$, and $d = -1$ for magnetic Bianchi Type VI₀, and ξ is a constant that depends on the strength of the magnetic field. In these models, the singularity occurs at $\tau = -\Omega = \infty$. From (8) and (9), we see that $V \rightarrow 0$ as $\tau \rightarrow \infty$ unless one of α , ζ , or γ is ≈ 0 . When the potential itself is small ($V \approx 0$), (7) describes a “free particle” in MSS and is in fact approximately the Kasner solution.

The standard algorithms for solving ODE's [25] often employ an adaptive time step. The idea is to take large time steps where nothing much happens (e.g. in the Kasner regime) while taking shorter time steps when the forces are large (e.g. at a bounce). Unfortunately, in Mixmaster dynamics, the duration of the Kasner epochs increases exponentially in τ as $\tau \rightarrow \infty$ [26] while the duration of the bounce itself is in some sense fixed [27]. This means that, although huge time steps may be taken in the Kasner segments, the time step must become very small at the bounces. Ideally, one would like the time step also to grow exponentially but this cannot be done with standard approaches. Thus, with a great deal of effort, standard methods can yield about 30 bounces for $0 < \tau < 10^8$ in about an hour on a supercomputer. The application of the symplectic method to Mixmaster dynamics is straightforward. From (7), we have

$$H_K = -p_\Omega^2 + p_+^2 + p_-^2 \quad ; \quad H_V = V(\Omega, \beta_+, \beta_-). \quad (10)$$

With an adaptive step size and a 6th order version of (5), one can do slightly better (approximately a factor of three fewer steps) than 4th order Runge-Kutta. However, it is well known that a bounce off an exponential wall—the Bianchi II (or Taub [4]) cosmology—is exactly solvable. If we first identify the dominant

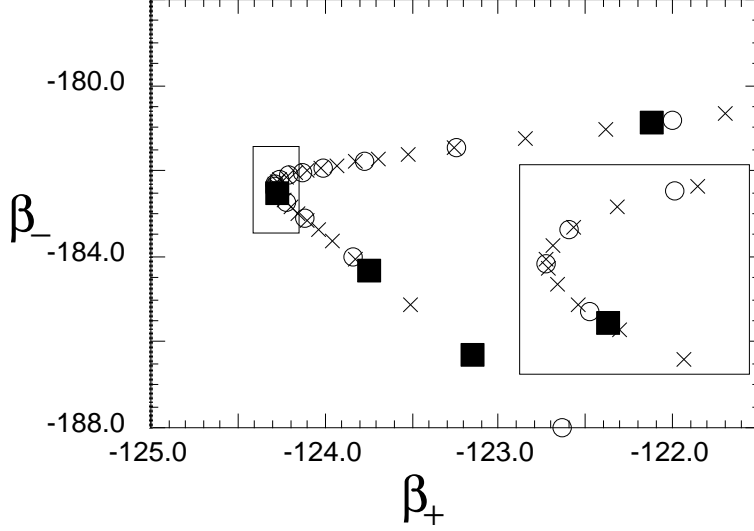


Figure 1: Comparison of algorithms for Mixmaster dynamics. A typical Mixmaster bounce is shown in the anisotropy plane. Crosses indicates every 10th point on a 4th order Runge-Kutta evaluation of the trajectory, while circles indicate every 10th point for a 6th order standard symplectic evaluation. The filled squares indicate *every* point using the new algorithm. The inset shows the details closest to the bounce. Note that the new algorithm does not require a point at the apex of the bounce.

exponential wall (say $e^{4\alpha}$), then we find that the symplectic algorithm works for a different split of the Hamiltonian into two subhamiltonians [20]. Let

$$H = H_1 + H_2 \quad (11)$$

where (e.g. for Bianchi IX)

$$H_1 = -p_\Omega^2 + p_+^2 + p_-^2 + e^{4\Omega - 8\beta_+} \quad ; \quad H_2 = H_V - e^{4\Omega - 8\beta_+}. \quad (12)$$

Variation of H_2 is exactly solvable as before, while variation of H_1 yields equations with solution

$$\begin{aligned} p_y(t + \Delta t) &= p_y(t) \quad ; \quad p_-(t + \Delta t) = p_-(t) \quad ; \\ y(t + \Delta t) &= y(t) - 6p_y(t)\Delta t \quad ; \quad \beta_-(t + \Delta t) = \beta_-(t) + 2p_-(t)\Delta t \quad ; \end{aligned}$$

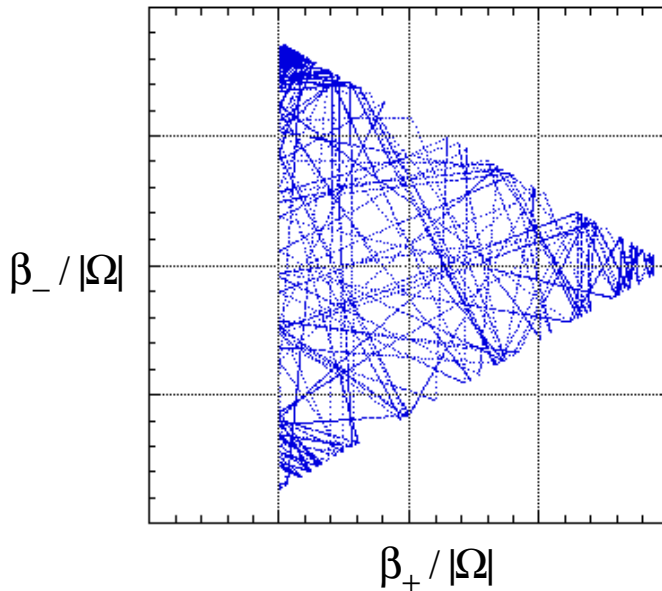


Figure 2: A typical trajectory consisting of 268 Mixmaster bounces is shown projected onto the anisotropy plane. In terms of the rescaled variables $\beta_+ / |\Omega|$ and $\beta_- / |\Omega|$, the walls of the MSS potential and thus the bounce sites are at fixed locations.

$$\alpha(t + \Delta t) = -\frac{1}{2} \ln \left[\frac{1}{E} \cosh 4\sqrt{3}(t + \Delta t - t_0) \right] ; \quad 6p_\alpha = \frac{d\alpha}{dt} \quad (13)$$

where $y = -2\Omega + \beta_+$ and $E^2 = 3p_y^2 - p_-^2$. This new symplectic algorithm provides an enormous advantage because the bounce is built in. The time step can grow exponentially. In a few minutes on a desktop computer, one can obtain, e.g., 268 bounces for $8 < \tau < 10^{61.5}$. Fig. 1 shows a comparison of the new and standard algorithms while Fig. 2 shows a typical trajectory. Since H_1 is actually the exact Hamiltonian almost all the time, the accuracy of the method is much higher than the formal 6th order—we achieve machine precision.

The BKL parameter u characterizes the angle in the anisotropy plane of the

Kasner epoch trajectory. Between the n th and $n + 1$ st Kasner epochs, we have

$$u_{n+1} = \begin{cases} u_n - 1 & ; \quad 2 \leq u_n < \infty \\ (u_n - 1)^{-1} & ; \quad 1 \leq u_n \leq 2 \end{cases} . \quad (14)$$

All numerical studies [5, 28, 29, 27] and a variety of analytic arguments [30, 20] have shown that one expects (14) to become ever more valid as $\tau \rightarrow \infty$. With our algorithm in a double or quadruple precision code, one can evolve until deviations from (14) disappear and then use the predicted values of u as a test of the accuracy of the code. For example [20], one discovers that the Hamiltonian constraint ((7) with $H = 0$) must be enforced although not necessarily at every time step.

For our studies of spatially inhomogeneous cosmologies, it is important to keep in mind that

(1) between bounces Mixmaster dynamics looks like the AVTD Kasner solution;

(2) in a fixed time variable such as τ , the time between bounces increases exponentially as $\tau \rightarrow \infty$;

(3) extraordinary accuracy can be achieved by symplectic methods when one of the subhamiltonians is dominant;

(4) enormous gains in accuracy and computational speed can be made by using a “custom-designed” treatment of the bounce.

4 The Gowdy Test Case

As the simplest example of a spatially inhomogeneous cosmology, we consider the plane symmetric vacuum Gowdy universe on $T^3 \times R$ [31, 32] described by the metric

$$ds^2 = e^{-\lambda/2} e^{\tau/2} (-e^{-2\tau} d\tau^2 + d\theta^2) + e^{-\tau} [e^P d\sigma^2 + 2e^P Q d\sigma d\delta + (e^P Q^2 + e^{-P}) d\delta^2] \quad (15)$$

where the background λ and amplitudes P and Q of the $+$ and \times polarizations of gravitational waves are functions of τ and $0 \leq \theta \leq 2\pi$ and periodic in θ . There is a curvature singularity at $\tau = \infty$ [32, 2, 33]. The polarized case ($Q = 0$) has been shown to have an AVTD singularity [2]. The generic case has been conjectured to be AVTD (except perhaps at a set of measure zero) [34], which we have verified to the extent possible numerically [21, 35, 36, 37, 38, 39, 22]. A claim has been made that this model does not have an AVTD singularity [40] which we believe to be incorrect [41].

This model is especially attractive as a test case because Einstein’s equations in our variables split into dynamical equations for the wave amplitudes (where

,_a = ∂/∂a):

$$P_{,\tau\tau} - e^{-2\tau} P_{,\theta\theta} - e^{2P} (Q_{,\tau}^2 - e^{-2\tau} Q_{,\theta}^2) = 0, \quad (16)$$

$$Q_{,\tau\tau} - e^{-2\tau} Q_{,\theta\theta} + 2 (P_{,\tau} Q_{,\tau} - e^{-2\tau} P_{,\theta} Q_{,\theta}) = 0 \quad (17)$$

while the Hamiltonian and momentum constraints become respectively first order equations for λ :

$$\lambda_{,\tau} - [P_{,\tau}^2 + e^{-2\tau} P_{,\theta}^2 + e^{2P} (Q_{,\tau}^2 + e^{-2\tau} Q_{,\theta}^2)] = 0, \quad (18)$$

$$\lambda_{,\theta} - 2(P_{,\theta} P_{,\tau} + e^{2P} Q_{,\theta} Q_{,\tau}) = 0. \quad (19)$$

Thus two problematical aspects of numerical relativity—preservation of the constraints and solution of the initial value problem—become trivial [31]. The wave equations (16) and (17) may be obtained by variation of the Hamiltonian

$$\begin{aligned} H &= \frac{1}{2} \int_0^{2\pi} d\theta [\pi_P^2 + e^{-2P} \pi_Q^2] \\ &+ \frac{1}{2} \int_0^{2\pi} d\theta [e^{-2\tau} (P_{,\theta}^2 + e^{2P} Q_{,\theta}^2)] = H_K + H_V \end{aligned} \quad (20)$$

where π_P and π_Q are canonically conjugate to P and Q respectively. Variation of H_K yields the AVTD solution

$$\begin{aligned} P &= \ln |\mu| + v(\tau - \tau_0) + \ln[1 + e^{-2v(\tau - \tau_0)}] \rightarrow v\tau \quad \text{as } \tau \rightarrow \infty, \\ Q &= Q_0 + \frac{1}{\mu} \frac{e^{-2v(\tau - \tau_0)}}{(1 + e^{-2v(\tau - \tau_0)})} \rightarrow Q_0 \quad \text{as } \tau \rightarrow \infty, \\ \pi_P &= v \frac{(1 - e^{-2v(\tau - \tau_0)})}{(1 + e^{-2v(\tau - \tau_0)})} \rightarrow v \quad \text{as } \tau \rightarrow \infty, \\ \pi_Q &= -2\mu v \end{aligned} \quad (21)$$

and is thus exactly solvable in terms of four functions of θ : μ , $v > 0$, Q_0 , and τ_0 . H_V is also (trivially) exactly solvable so that symplectic methods can be used [21].

If the singularity is AVTD, one would expect the spatial derivative terms to go to zero exponentially as $\tau \rightarrow \infty$. However, if $P \rightarrow v\tau$, the term

$$V_2 = e^{-2\tau + 2P} Q_{,\theta}^2 \quad (22)$$

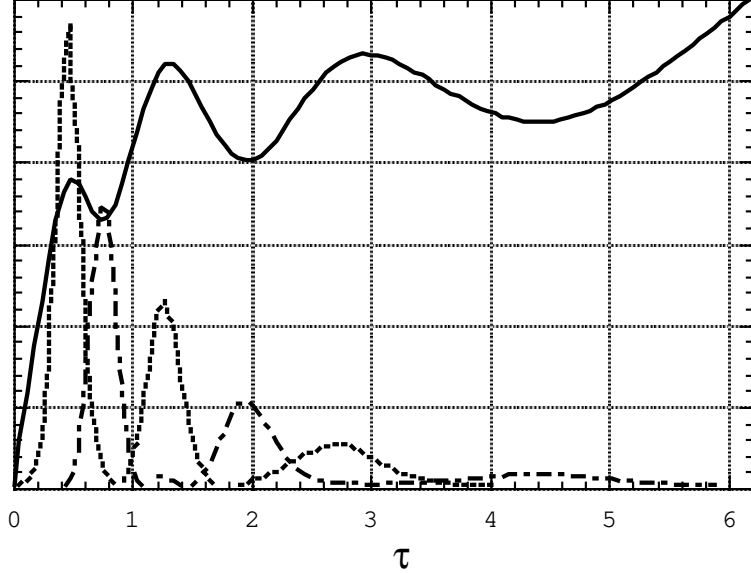


Figure 3: P (solid curve), V_1 (dash-dotted curve), and V_2 (dashed curve) vs τ at a fixed value of θ . Note that the slope of P , $P_{,\tau}$, decreases after each interaction with V_2 while $P_{,\tau}$ goes from negative to positive after each interaction with V_1 . A continuation of this graph in τ would show that V_1 and V_2 have permanently died off and that P continues to increase with fixed positive slope $P_{,\tau} < 1$.

in (16) would grow rather than decay if $v > 1$. Thus Grubišić and Moncrief (GM) [34] conjectured that, in a generic Gowdy model as $\tau \rightarrow \infty$, $0 \leq v < 1$ except perhaps at isolated spatial points. If we consider generic initial data—e.g. $P = 0$, $\pi_P = v_0 \cos \theta$, $Q = \cos \theta$, $\pi_Q = 0$ —then we must ask how a generic Gowdy solution evolves toward the AVTD solution at each spatial point and how an initial $P_{,\tau} > 1$ or $P_{,\tau} < 0$ is brought into the conjectured range. Typically, either V_2 or

$$V_1 = \pi_Q^2 e^{-2P} \quad (23)$$

(where $\pi_Q = e^{2P} Q_{,\tau}$) will dominate (16) to yield either

$$P_{,\tau}^2 + \pi_Q^2 e^{-2P} \approx \kappa_1^2 \quad (24)$$

or

$$Z_{,\tau}^2 + Q_{,\theta}^2 e^{2Z} \approx \kappa_2^2 \quad (25)$$

where $Z = P - \tau$. If $P_{,\tau} < 0$, an interaction with V_1 will occur to drive $P_{,\tau}$ to $-P_{,\tau}$ to yield $P_{,\tau} > 0$. If $P_{,\tau} > 1$, an interaction with V_2 will occur to drive

$(P_{,\tau} - 1)$ to $-(P_{,\tau} - 1)$. If this yields $P_{,\tau} < 0$, a second interaction with V_1 will occur, etc. When $|P_{,\tau}| < 1$, V_2 disappears so that, after a possible final interaction with V_1 , $0 \leq P_{,\tau} < 1$ forever. A typical sequence of bounces is shown in Fig. 3. Fig. 4 shows the maximum value of v on the spatial grid vs τ . First

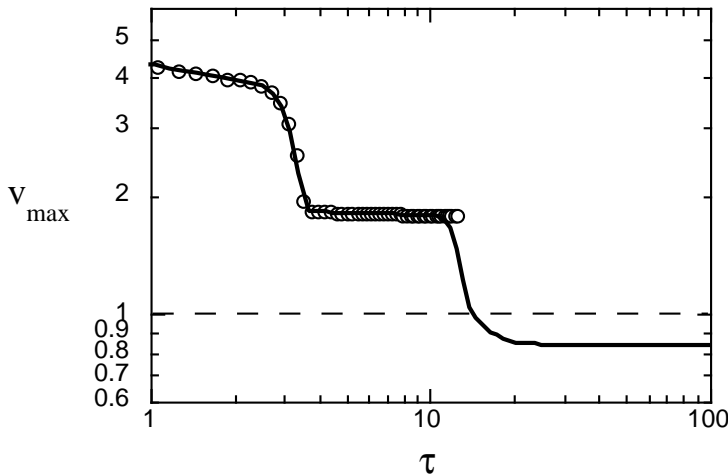


Figure 4: Plot of v_{max} vs τ . The maximum value of v is found for two simulations with 3200 (solid line) and 20000 spatial grid points (circles) respectively. The horizontal line indicates $v = 1$. Continuation in τ of the finer resolution simulation would show $v_{max} > 1$ for a much longer τ with $v_{max} < 1$ eventually.

we see that high values of τ can be reached at which $0 \leq v < 1$ everywhere.

Non-generic behavior can occur at isolated spatial points where either π_Q or $Q_{,\theta}$ vanishes. In the former case, the absence of V_1 where $\pi_Q = 0$ and its flatness where $\pi_Q \approx 0$ allow $P_{,\tau}$ and thus P to remain negative for a long time. Since $Q_{,\tau} = \pi_Q e^{-2P}$, Q will grow exponentially in opposite directions on either side of the points where $\pi_Q = 0$ producing a characteristic apparent discontinuity. On the other hand, if $Q_{,\theta} \approx 0$, $P_{,\tau}$ can remain large for a long time causing a spiky feature in P . Both types of features sharpen and narrow with time. The features and their association with non-generic points are shown in Fig. 5. The presence of this non-generic behavior at isolated spatial points leads to a dependence of simulation results on the spatial resolution. The finer the spatial resolution, the closer will a grid point be to the non-generic point. Near these non-generic points, the generic process of approach to $0 \leq P_{,\tau} < 1$ will occur but slowly since either π_Q or $Q_{,\theta} \approx 0$. The closer one is to a non-generic site, the longer this process will take. Thus a finer resolution code will have narrower spiky features at which it takes longer for $P_{,\tau}$ to move into the range $[0, 1)$. Some

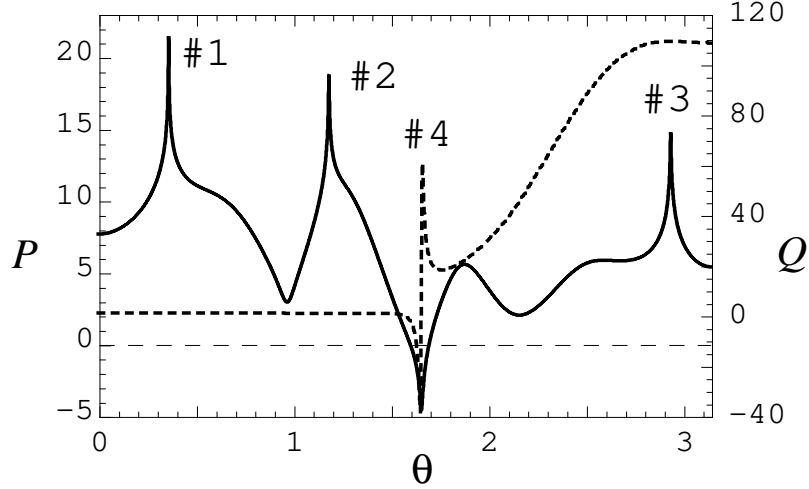


Figure 5: P (solid line) and Q (dashed line) vs θ at $\tau = 12.4$ for the initial data set given here with $v_0 = 5$ for $0 \leq \theta \leq \pi$ for a simulation containing 20000 spatial grid points in the interval $[0, 2\pi]$. The numbers on the graph refer to the most interesting features. Peaks #1, #2, and #3 in P are essentially the same in that they occur where $Q_{,\theta} \approx 0$. Peak #4 shows an apparent discontinuity in Q where $\pi_Q \approx 0$.

evidence for this is seen in Fig. 4 where the finer spatial resolution simulation diverges from the coarser one and will be considered in detail elsewhere [22].

Finally, we note that V_2 is analogous to the MSS potential. One may consider then application of the new Mixmaster algorithm to the Gowdy Hamiltonian (20) with $H = H_1 + H_2$ for

$$H_1 = \frac{1}{2} \oint d\theta (\pi_P^2 + e^{-2\tau+2P} Q_{,\theta}^2) \quad (26)$$

and

$$H_2 = \frac{1}{2} \oint d\theta (\pi_Q^2 e^{-2P} + e^{-2\tau} P_{,\theta}^2). \quad (27)$$

These yield the exact solutions

$$Q(\tau + \Delta\tau) = Q(\tau),$$

$$\pi_Q(\tau + \Delta\tau) = \xi + \left[\frac{\kappa}{Q(\tau)_{,\theta}} \tanh \kappa(\tau - \tau_0) \right]_{,\theta},$$

$$\begin{aligned}
P(\tau + \Delta\tau) &= \tau - \ln \left[\left| \frac{Q(\tau),\theta}{\kappa} \right| \cosh \kappa(\tau - \tau_0) \right], \\
\pi_P(\tau + \Delta\tau) &= 1 - |\kappa| \tanh \kappa(\tau - \tau_0)
\end{aligned} \tag{28}$$

from the variation of H_1 (where ξ , κ , and τ_0 are functions of θ) and

$$\begin{aligned}
P(\tau + \Delta\tau) &= P(\tau), \\
\pi_Q(\tau + \Delta\tau) &= \pi_Q(\tau), \\
\pi_P(\tau + \Delta\tau) &= \pi_P(\tau) + \pi_Q^2(\tau) e^{-2P(\tau)} \Delta\tau + \frac{1}{2} e^{-2\tau} (1 - e^{-2\Delta\tau}) P(\tau),_{\theta\theta} , \\
Q(\tau + \Delta\tau) &= Q(\tau) + \pi_Q(\tau) e^{-2P(\tau)} \Delta\tau
\end{aligned} \tag{29}$$

from the variation of H_2 . Application of this algorithm is in progress.

From the Gowdy test case, we learn that:

(1) Since the singularity is AVTD, H_K dominates H_V asymptotically so our (current) algorithm is very accurate.

(2) Non-linear terms in the wave equations act as potentials. In the Gowdy case, they drive the system to the AVTD regime as $\tau \rightarrow \infty$ with $0 \leq v < 1$, where the potentials permanently die out.

(3) Non-generic points where $\pi_Q = 0$ or $Q,_{\theta} = 0$ lead to the growth of spiky features in P and Q .

(4) Spiky features appear narrower with finer spatial resolution.

5 $U(1)$ Symmetric Cosmologies

Given our understanding of the Gowdy model, we can move to spatially inhomogeneous cosmologies with one Killing field rather than two, retaining a $U(1)$ symmetry on $T^3 \times R$ [42]. These models can be described by five degrees of freedom $\{\varphi, \omega, \Lambda, z, x\}$ and their respective conjugate momenta $\{p, r, p_\Lambda, p_z, p_x\}$ which are functions of spatial variables u and v and time τ . Einstein's equations may be obtained by variation of [21, 23]

$$\begin{aligned}
H &= \oint \oint du dv \mathcal{H} \\
&= \oint \oint du dv \left(\frac{1}{8} p_z^2 + \frac{1}{2} e^{4z} p_x^2 + \frac{1}{8} p^2 + \frac{1}{2} e^{4\varphi} r^2 - \frac{1}{2} p_\Lambda^2 + 2p_\Lambda \right) \\
&\quad + e^{-2\tau} \oint \oint du dv \left\{ (e^\Lambda e^{ab}),_{ab} - (e^\Lambda e^{ab}),_a \Lambda_{,b} + e^\Lambda [(e^{-2z}),_u x_{,v} - (e^{-2z}),_v x_{,u}] \right\}
\end{aligned}$$

$$\begin{aligned}
& + 2e^\Lambda e^{ab} \varphi_{,a} \varphi_{,b} + \frac{1}{2} e^\Lambda e^{-4\varphi} e^{ab} \omega_{,a} \omega_{,b} \} \\
= & H_K + H_V = \oint \oint du dv \mathcal{H}_K + \oint \oint du dv V. \tag{30}
\end{aligned}$$

Here φ and ω are analogous to P and Q while Λ, x, z describe the metric \tilde{e}_{ab} in the u - v plane perpendicular to the symmetry direction with

$$\tilde{e}_{ab} = e^{2\Lambda} e_{ab} = \frac{1}{2} e^{2\Lambda} \begin{pmatrix} e^{2z} + e^{-2z}(1+x)^2 & e^{2z} + e^{-2z}(x^2-1) \\ e^{2z} + e^{-2z}(x^2-1) & e^{2z} + e^{-2z}(1-x)^2 \end{pmatrix}. \tag{31}$$

This model is sufficiently generic that local Mixmaster dynamics is allowed. The $U(1)$ Hamiltonian (30) has the standard symplectic form. Note that H_K consists of two Gowdy-like H_K 's and a free particle term so that H_K is exactly solvable. H_V is also (again trivially) exactly solvable although spatial differencing must be performed with care. In two spatial dimensions, there are a variety of ways to represent derivatives to a given order of accuracy. We currently use a scheme provided by Norton [43] to minimize the growth of short wavelength modes.

Unlike the Gowdy model, the constraints and initial value problems must be considered. We find

$$\mathcal{H}^0 = \mathcal{H} - 2p_\Lambda = 0 \tag{32}$$

and

$$\begin{aligned}
\mathcal{H}^u & = p_z z_{,u} + p_x x_{,u} + p_\Lambda \Lambda_{,u} - p_{\Lambda,u} + p \varphi_{,u} + r \omega_{,u} \\
& + \frac{1}{2} \{ [e^{4z} - (1+x)^2] p_x - (1+x)p_z \}_{,v} \\
& - \frac{1}{2} \{ [e^{4z} + (1-x)^2] p_x - x p_z \}_{,u} = 0, \tag{33}
\end{aligned}$$

$$\begin{aligned}
\mathcal{H}^v & = p_z z_{,v} + p_x x_{,v} + p_\Lambda \Lambda_{,v} - p_{\Lambda,v} + p \varphi_{,v} + r \omega_{,v} \\
& - \frac{1}{2} \{ [e^{4z} - (1-x)^2] p_x + (1-x)p_z \}_{,u} \\
& + \frac{1}{2} \{ [e^{4z} + (1-x^2)] p_x - x p_z \}_{,v} = 0. \tag{34}
\end{aligned}$$

While a general solution to the initial value problem is not known, we use the particular solution obtained as follows: To solve the momentum constraints (33) and (34) set $p_x = p_z = \varphi_{,a} = \omega_{,a} = 0$ to leave $p_\Lambda \Lambda_{,a} - p_{\Lambda,a} = 0$ which may be satisfied by requiring $p_\Lambda = c e^\Lambda$. For sufficiently large c , the Hamiltonian

constraint may be solved algebraically for either p or r . In general, this leaves as free data the four functions x , z , Λ , and either r or p . Since there are four free functions at each spatial point, we expect generic behavior.

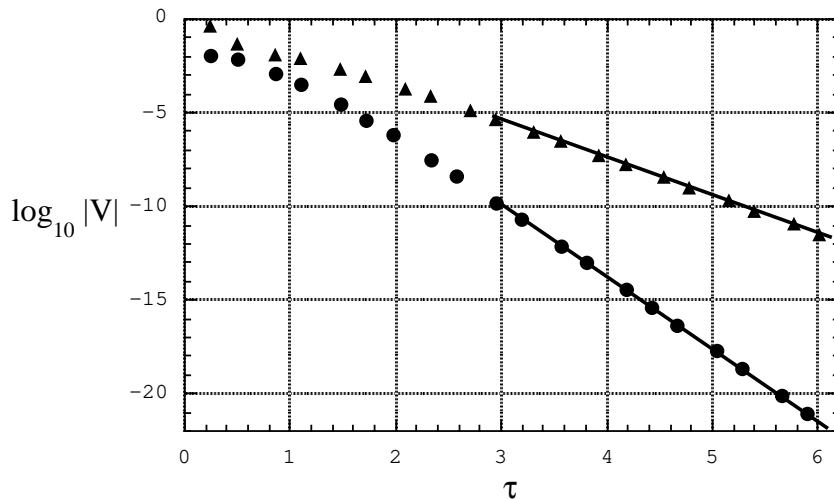


Figure 6: Evolution of $\log_{10}|V|$ vs τ for a polarized $U(1)$ cosmology at two representative spatial points. The solid lines are exponential fits.

As a first case, we consider polarized $U(1)$ models obtained by setting

$$r = \omega = 0. \quad (35)$$

This condition is preserved numerically as well as analytically. It has been conjectured [44] that polarized $U(1)$ models are AVTD. This is reasonable because the Mixmaster potential-like term

$$V_{\nabla\omega} = e^{-2\tau} e^{\Lambda} e^{ab} e^{-4\varphi} \omega_{,a} \omega_{,b} \quad (36)$$

is absent. Other spatial derivative terms decay as $e^{\Lambda-2\tau-2z}$ for the expected AVTD limits of the variables as $\tau \rightarrow \infty$ [23]:

$$\begin{aligned} z &\rightarrow -v_z \tau, & x &\rightarrow x_0, & p_z &\rightarrow -v_z, \\ p_x &\rightarrow p_x^0, & \varphi &\rightarrow -v_\varphi \tau, & p &\rightarrow -v_\varphi, \\ \Lambda &\rightarrow \Lambda_0 + (2 - p_\Lambda^0) \tau, & p_\Lambda &\rightarrow p_\Lambda^0, \end{aligned} \quad (37)$$

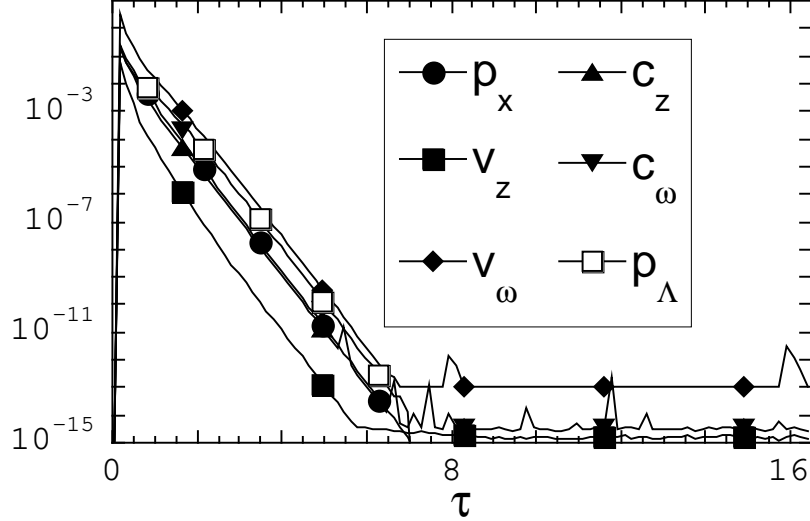


Figure 7: The **maximum** value of the **change** with time over the spatial grid of AVTD regime constants for a polarized $U(1)$ symmetric model. Here $v_z = \sqrt{p_z^2/8 + e^{4z}p_x^2/2}$, $v_\omega = \sqrt{p^2/8 + e^{4\varphi}r^2/2}$, $c_z = p_z/2 + p_x x$, and $c_\omega = p/2 + r\omega$. Exponential decay is observed until the maximum values of the changes reach the level of machine precision.

so that an AVTD singularity is consistent.

Fig. 6 shows $\log_{10}|V|$ vs τ for typical spatial points. Thus we see the expected exponential decay. In Fig. 7, we see that the maximum values of the changes with time of the quantities expected to be constant in an AVTD regime also decay exponentially as expected. These results will be discussed in detail elsewhere [23].

We emphasize here that the polarized $U(1)$ models present *no* numerical difficulties. The absence of $V_{\nabla\omega}$ means that spiky features do not develop. The situation unfortunately changes for generic (unpolarized) $U(1)$ models. It appears that consistency arguments which suggest an AVTD singularity in polarized $U(1)$ models and restrict v to $[0, 1]$ in the Gowdy models fail in generic $U(1)$ models. This suggests that $V_{\nabla\omega}$ will always grow exponentially if the system tries to be AVTD producing a Mixmaster-like bounce. A bounce in the opposite direction will come, as in Gowdy models, from terms in H_K . This bouncing could continue indefinitely.

Unfortunately, the bounces off $V_{\nabla\omega}$ probably cause numerical instabilities that limit the duration of the simulations. Spatial averaging has been used

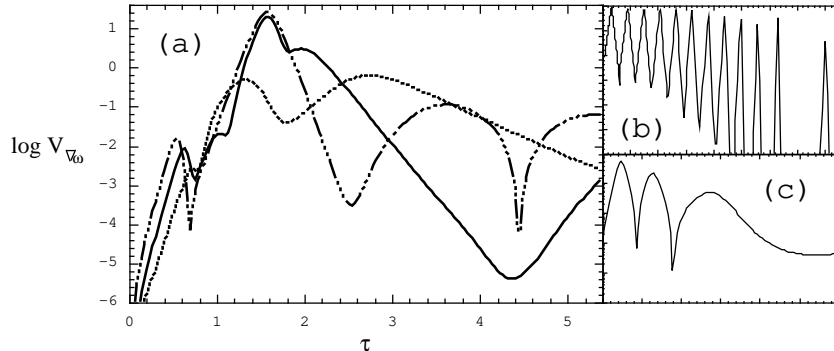


Figure 8: (a) $\log_{10} V$ vs τ for three representative spatial points of a generic $U(1)$ symmetric cosmology. (b) The analogous quantity for a typical Mixmaster evolution. (c) The analogous quantity for a Gowdy simulation.

to improve stability but it is known to produce numerical artifacts. Typical evolutions of $V_{\nabla\omega}$ at single spatial grid points are shown in Fig. 8 and compared to similar quantities in Mixmaster and Gowdy models and, of course, to Fig. 6. While generic $U(1)$ models are clearly different from polarized ones, it is not clear yet whether the observed bounces are Mixmaster-like or will eventually die out as in Gowdy models. Recall that Mixmaster universes are very close to the AVTD Kasner solution between bounces. One is also concerned about numerical artifacts although it is not clear that standard tests are helpful. Fig. 9 shows two frames from a movie of $V(u, v)$ vs τ for two different spatial resolutions. Features are narrower on the finer grid. While this usually indicates artifacts, we recall that this is precisely what happens in Gowdy models where the resolution dependence is well understood.

6 Future Directions

In the search for the nature of the generic cosmological singularity, we have obtained convincing evidence that both the Gowdy universes and the polarized $U(1)$ symmetric cosmologies have AVTD singularities. These results are found in simulations which present no numerical difficulties. In contrast, we cannot draw definite conclusions for generic $U(1)$ models except to say that we have not found evidence that the singularities are AVTD everywhere.

Presumably, numerical difficulties in generic $U(1)$ models are due to Gowdy-like spiky features (which are less easy to represent accurately in two spatial dimensions). It is possible that the new Mixmaster algorithm [20] which can

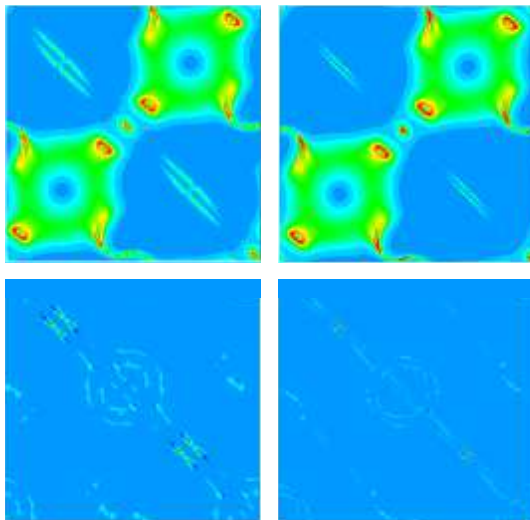


Figure 9: Movie frames of $V(u, v)$ for a generic $U(1)$ symmetric cosmology for two fixed values of τ . The upper frames precede the lower ones. The spatial coordinates u and v run from 0 to 2π in both directions. The frames on the left are from a simulation with 128^2 spatial grid points while the ones on the right have 256^2 spatial grid points. Both simulations have the same initial data. Note that there are features independent of spatial resolution as well as those that depend on the resolution. The background shade of gray indicates regions where $V \approx 0$.

be adapted to the Gowdy model will help in the generic $U(1)$ case where it can also be implemented. The hope is that better treatment of the bounces would give better local treatment of spiky features that arise from them.

While we solve the constraints initially in $U(1)$ models, we do nothing to preserve them thereafter. In the polarized case, they remain acceptably small (and in fact converge to zero with increasing spatial resolution). We have learned from the Mixmaster case that one must preserve the constraints [20]. In fact, it is the kinetic part of the Hamiltonian constraint which restricts the exponential factor in $V_{\nabla\omega}$. An error in the constraints could give the argument of the exponential the wrong sign leading to the observation of qualitatively wrong behavior. By starting closer to the singularity, we can suppress some of the

numerical instabilities and study this controlling exponential. Studies of this type have provided some evidence that it is essential to solve the constraints. Work on implementing a constraint solver is in progress.

Acknowledgements

B.K.B. and V.M. would like to thank the Albert Einstein Institute at Potsdam for hospitality. B.K.B. would also like to thank the Institute of Geophysics and Planetary Physics of Lawrence Livermore National Laboratory for hospitality. This work was supported in part by National Science Foundation Grants PHY9507313 and PHY9722039 to Oakland University and PHY9503133 to Yale University. Computations were performed at the National Center for Supercomputing Applications (University of Illinois).

References

- [1] D. Eardley, E. Liang, R. Sachs, *J. Math. Phys.* **13**, 99 (1972).
- [2] J. Isenberg, V. Moncrief, *Ann. Phys. (N.Y.)* **199**, 84–122 (1990).
- [3] E. Kasner, *Am. J. Math* **43**, 130 (1921).
- [4] A. Taub, *Ann. Math.* **53**, 472 (1951).
- [5] V.A. Belinskii, E.M. Lifshitz, I.M. Khalatnikov, *Sov. Phys. Usp.* **13**, 745–765 (1971); *Adv. Phys.* **19**, 525–573 (1970).
- [6] C.W. Misner, *Phys. Rev. Lett.* **22**, 1071–1074 (1969).
- [7] P. Halpern, *J. Gen. Rel. Grav.* **19**, 73–94 (1987).
- [8] V.G. LeBlanc, D. Kerr, J. Wainwright, *Class. Quantum Grav.* **12**, 513 (1995).
- [9] B.K. Berger, *Class. Quantum Grav.* **13**, 1273–1276 (1996).
- [10] V.G. LeBlanc, *Class. Quantum Grav.* **14**, 2281–2301 (1997).
- [11] R.T. Jantzen, *Phys. Rev. D* **33**, 2121 (1986).
- [12] N.J. Cornish, J.J. Levin, *Phys.Rev.Lett.* **78**, 998–1001 (1997)
- [13] M.P. Ryan, Jr., L.C. Shepley, *Homogeneous Relativistic Cosmologies* (Princeton University, Princeton,1975).
- [14] J.D. Barrow, F. Tipler, *Phys. Rep.* **56** 372 (1979).
- [15] G. Montani, *Class. Quantum Grav.* **12**, 2505 (1995).

- [16] V.A. Belinskii, *JETP Lett.* **56**, 421 (1992).
- [17] A.A. Kirillov, A.A. Kochnev, *JETP Lett.* **46**, 435 (1987); A.A. Kirillov, *JETP* **76**, 355 (1993).
- [18] J.A. Fleck, J. R. Morris, M.D. Feit, *Appl. Phys.* **10**, 129–160 (1976).
- [19] V. Moncrief, *Phys. Rev. D* **28**, 2485–2490 (1983).
- [20] B.K. Berger, D. Garfinkle, E. Strasser, *Class. Quantum Grav.* **14**, L29–L36 (1997).
- [21] B.K. Berger, V. Moncrief, *Phys. Rev. D* **48**, 4676 (1993).
- [22] B.K. Berger, D. Garfinkle, B. Grubišić, V. Moncrief, “Phenomenology of the Gowdy Cosmology on $T^3 \times R$ ”, unpublished.
- [23] B.K. Berger, V. Moncrief, “Numerical Evidence for a Velocity Dominated Singularity in $U(1)$ Symmetric Cosmologies,” unpublished.
- [24] M. Suzuki, *Phys. Lett.* **A146**, 319 (1990).
- [25] W.H. Press, B.P. Flannery, S.A. Teukolsky, W.T. Vetterling, *Numerical Recipes: the Art of Scientific Computing (2nd edition)* (Cambridge University, Cambridge, 1992).
- [26] I.M. Khalatnikov, E.M. Lifshitz, K.M. Khanin, L.N. Shchur, and Ya. G. Sinai, *J. Stat. Phys.* **38**, 97–114 (1985).
- [27] B.K. Berger, *Gen. Rel. Grav.* **23**, 1385–1402 (1991).
- [28] A.R. Moser, R.A. Matzner, M.P. Ryan, Jr., *Ann. Phys. (N.Y.)* **79**, 558–579 (1973).
- [29] S.E. Rugh, Cand. Scient. Thesis, Niels Bohr Inst. (1990); S.E. Rugh, B.J.T. Jones, *Phys. Lett.* **A147**, 353 (1990).
- [30] A.D. Rendall, *Class. Quantum Grav.* **14**, 2341–2356 (1997).
- [31] R.H. Gowdy, *Phys. Rev. Lett.* **27**, 826–829 (1971).
- [32] B.K. Berger, *Ann. Phys. (N.Y.)* **83**, 458 (1974).
- [33] V. Moncrief, *Ann. Phys. (N.Y.)* **132**, 87–107 (1981).
- [34] B. Grubišić, V. Moncrief, *Phys. Rev. D* **47**, 2371 (1993).
- [35] B.K. Berger, D. Garfinkle, B. Grubisic, V. Moncrief, V. Swamy, in *Proceedings of the Cornelius Lanczos Symposium*, edited by J.D. Brown, M.T. Chu, D.C. Ellison, R.J. Plemmons (SIAM, Philadelphia, 1994).

- [36] B.K. Berger, D. Garfinkle, V. Moncrief, C.M. Swift, in *Proceedings of the AMS-CMS Special Session on Geometric Methods in Mathematical Physics*, ed. by J. Beem and K. Duggal (American Mathematical Society, 1994).
- [37] B.K. Berger, in *Seventh Marcel Grossmann Meeting*, edited by R. Ruffini, M. Keiser (World Scientific, Singapore, 1995).
- [38] B.K. Berger, in *Relativity and Scientific Computing*, edited by F.W. Hehl, R.A. Puntigam, H. Ruder (Springer-Verlag, Berlin, 1996).
- [39] B.K. Berger, in *Proceedings of the 14th International Conference on General Relativity and Gravitation*, edited by M. Francaviglia, G. Longhi, L. Lusanna, E. Sorace (World Scientific, Singapore, 1997).
- [40] S.J. Hern, J.M. Stewart, “The Gowdy T^3 Cosmologies Revisited,” gr-qc/9708038.
- [41] B.K. Berger, D. Garfinkle, V. Moncrief, “Comment on ‘The Gowdy T^3 Cosmology Revisited’,” gr-qc/9708050.
- [42] V. Moncrief, *Ann. Phys. (N.Y.)* **167**, 118 (1986).
- [43] A. Norton, private communication
- [44] B. Grubišić, V. Moncrief, *Phys. Rev. D* **49**, 2792 (1994).